Journal of Magnetics 11(4), 182-188 (2006)

<Invited review paper>

The Effect of Cr Dosage on FePt Nanoparticle Formation

C. Won[1]*, D. J. Keavney[2], R. Divan[3], and S. D. Bader[1,3]

[1]*Material Science Division, Argonne National Laboratory, Argonne, Illinois 60439*
[2]*Advanced Photon Source, Argonne National Laboratory, Argonne, Illinois 60439*
[3]*Center for Nanoscale Materials, Argonne National Laboratory, Argonne, Illinois 60439*

(Received 8 November 2006)

The search for high-density recording materials has been one of most active and vigorous field in the field of magnetism. FePt-$L1_0$ nanoparticle has emerged as a potential candidate because of its high anisotropy. In this paper, we provide an overview of recent work at Argonne National Laboratory that contributes to the ongoing dialogue concerning the relation between structure and properties of the FePt nanoparticle system. In particular we discuss the ability to control structure and properties via dosing with Cr. Cr-dosed FePt films were grown via molecular beam epitaxy and annealed at 550°C in an ultrahigh vacuum chamber, and were studied with the surface magneto-optic Kerr effect (SMOKE), scanning electron microscopy (SEM) and x-ray magnetic circular dichroism (XMCD). We found that small dosage of Cr helps to generate $L1_0$ phase FePt magnetic nanoparticles with small size, defined shape and regular spatial distribution on MgO (001) substrate. The nanostructures are ferromagnetic with high magnetic coercivity (~0.9T) and magnetic easy axis in the desired out-of-plane orientation. We also show that controlling the lateral region where nanostructures exist is possible via artificial patterning with Cr.

Keywords : FePt, Cr, L10 structure, SMOKE, XMCD, perpendicular anisotropy, spin reoreintation transition

1. Introduction

The search for high-density recording media has become a vigorous area of material science research. Magnetic nanoparticles have attracted great interest as potential candidates [1]. Especially, the $L1_0$ phase of FePt [2-9] has received much attention due to its high magnetocrystalline anisotropy ($K_u \cong 7.0 \times 10^6$ J/m^3). A high value of K_u prevents spin fluctuations due to thermal activation. Studies have focused on the fabrication of FePt $L1_0$ nanoparticles to make structures of controlled shape and size with a regular spatial distribution, while maintaining a high coercivity [10-13]. There are generally two methods to make FePt nanoparticles: one is chemical synthesis [10, 11] and the other is thin film deposition [4-6]. FePt nanoparticles made by chemical synthesis have a good size distribution and a regular shape, though magnetically they are weaker than those made by thin film deposition. The nanoparticles made via chemical synthesis can be well stacked and can form three dimensional (3D) superlattices [10]. However a 2D monolayer of nanoparticles are agglomerated one another, hence the spatial distribution is relatively poor and the magnetic easy axis of the particles is random [11, 14, 15]. In the synthesis of $L1_0$ FePt via thin film deposition, FePt films are deposited by RF sputtering or thermal evaporation in a vacuum chamber. Room-temperature-grown FePt without a subsequent annealing process yields the A1 phase alloy. This phase is disordered and there is a high energy barrier between the disordered and ordered phase [16]. After annealing, the FePt becomes $L1_0$ phase, which consists of alternate stacks of Fe and Pt. Many factors, such as the atomic ratio between Fe and Pt, growth temperature, anneal temperature, substrate, and deposition method affect the structure, size, and shape of the FePt film [17-19]. Addition of non-magnetic material to FePt is known to provide an efficient way to enhance the magnetic properties due to the segregation of non-magnetic solute atoms at grain boundaries [20-26]. Most vacuum deposited FePt films exhibit a granular surface composed of nanostructures of various sizes and shapes. However, the value of the magnetic coercivity (H_c) is higher than that made by chemical synthesis, reaching up to 7T [27]. Recently, nanoparticle

*Corresponding author: Tel: +1-630-252-5650,
Fax: +1-630-252-9595, e-mail: won@anl.gov

generation has been reported in some studies with conventional vacuum deposition techniques [28-30]; however, a substrate heating > 700°C was required and the particle-size distribution was not well controlled.

In work at Argonne National Laboratory, we highlight that we find that a small dosage of Cr on FePt at room temperature helps to generate circularly shaped $L1_0$ FePt particles after annealing at 550°C. The particle diameter is ~15 nm and the coercivity is ~0.9 T. We found there is a phase separation between flat and planar A1 phase FePt and round $L1_0$ phase FePt magnetic particles. As the dosage of Cr increases, the fraction of A1 phase increases and whole surface becomes planar phase and the magnetic easy axis changes from out-of-plane to in-plane around 2 Cr atoms/lattice site at both 1.8- and 3.6-nm FePt thicknesses. We believe small dosage of Cr makes the $L1_0$ FePt circular, and abundant Cr is segregated to the planar FePt phase. We also highlight results with FePt films grown on a Cr patterned substrate, and show the arbitrary tailoring of both phases is possible by pre-patterning with Cr.

2. Experiments

Samples were deposited in an ultrahigh vacuum chamber with a base pressure of 1×10^{-10} Torr. Fe (0.16 nm) and Pt (0.2 nm) layers were alternately deposited by e-beam evaporators at room temperature on MgO substrate. Alternate deposition with one layer thickness was reported to enhance the order of the structure and the lower annealing temperature required for the structural transition from the disordered A1 to the ordered $L1_0$ phase [19]. Cr was dosed two different ways. In one kind of samples, Cr ad-layers were deposited with a wedge shape to change the Cr dosage continuously. The size of a wedge is of order of a millimeter and the dosage range is from zero to 0.5 nm; the slope is only ~0.1 nm/mm, so the variance of Cr dosage in a measurement spot is negligible, considering a measurement spot size is < 0.1 mm. In the other kind of samples, Cr was pre-patterned on an MgO substrate before the growth of the FePt (Fig. 1). In the first type of samples, the Cr wedge was created by moving a sample behind a shutter during the Cr deposition, and in the second type of samples, Cr patterns were made by depositing Cr through a SiN mask made by e-beam lithography (Raith 150), RIE (Plasma Science 600) and wet chemical etching. Cr layers were deposited at room temperature. Typical deposition rates were 6 nm/hr for Fe and 1 nm/hr for Pt, which was monitored before and after deposition using a quartz crystal thickness monitor. The films were annealed after the final deposition at 350-

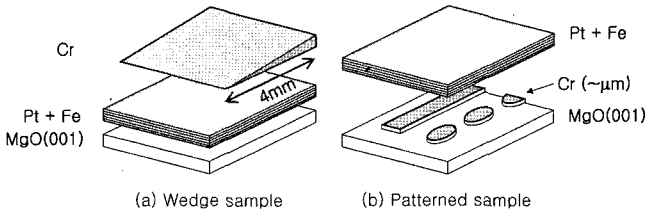

Fig. 1. Schematics of the dosage sequence and sample geometry. (a) Cr wedges were grown onto Fe(0.16 nm)/Pt(0.2 nm) multilayer films on 6-mm MgO(001) substrates. (b) FePt multilayer films grown on Cr-patterned MgO substrate.

to -550°C for 15 minutes in the ultrahigh vacuum chamber until there were no changes in the reflection high-energy election diffraction (RHEED) patterns. Magnetic properties were measured *in situ* by means of SMOKE, using a focused HeNe laser (633 nm wavelength). The films were then capped with 2 nm of Ag both for protection and electrical conduction. The capping layers were grown at room temperature and were not subject to any heat treatment. The samples were transferred in air to the x-ray magnetic circular dichroism (XMCD) chamber at beamline 4-ID-C of the Advanced Photon Source at Argonne National Laboratory. Topological structures were studied via SEM (LEO software). All measurements have been done at room temperature.

3. Results and Discussion

Figure 2 shows experimental results of a Cr-wedge sample of which the FePt thickness is 1.8 nm, which corresponds to 5 stacks of each atomic Fe and Pt layer. The first row shows the RHEED patterns on 0, 0.1 and 0.4 nm of Cr-dosed surface. The direction of the electron beam is along the <100>, which is perpendicular to the Cr wedge direction. The geometry was chosen in order to separate the RHEED pattern of each thickness of Cr. The RHEED images in Fig. 2 were taken after the sample cooled back to room temperature after annealing. The RHEED pattern without Cr dosage shows streaks along with dots whose distance correspond either to the lattice constant of FePt $L1_0$ phase (double layer distance) or one half of it (a layer distance). The spot associated with the double layer distance cannot be seen in the A1 disordered structure because of destructive interference in the diffraction pattern. Thus, superlattice spots show that there exists L10 order, which corresponds to alternate repetition of Fe and Pt layers along the surface normal direction [9]. The existence of RHEED spots also means that the surface of the film is not flat and is composed of 3D structures. With a small amount of Cr dosage, the RHEED

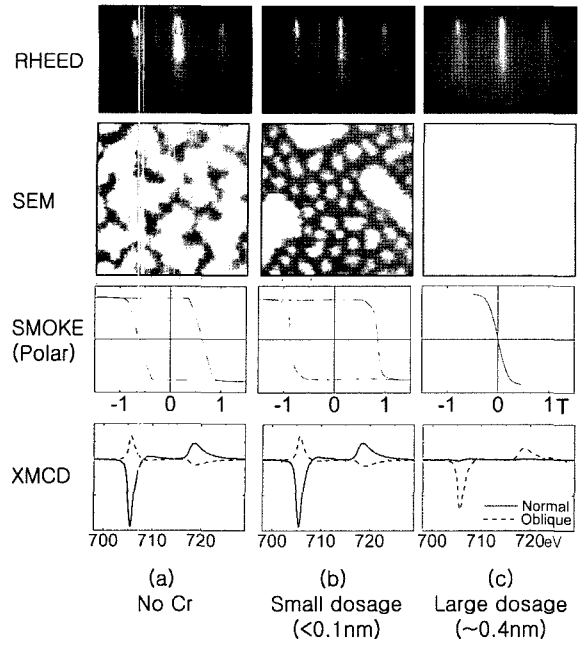

Fig. 2. RHEED, SEM, SMOKE, and XMCD results of 1.8-nm FePt film with (a) no Cr (b) small Cr and (c) large Cr dosed 1.8-nm FePt film after 550°C annealing. The size of the SEM image is 200×200 nm. (Magnification ratio is around 100,000).

pattern gets sharper while maintaining the original basic features ($L1_0$ order/3D structures). The sharpening suggests that a small amount of Cr makes the crystalline structure better than that of the pure film. The superlattice spots fade away for the ~0.4-nm thick Cr and the streaks sharpen further [Fig. 2(c)]. These results suggest that a large amount of Cr makes the film flat without inducing 3D structures. The second panel of Fig. 2 shows the SEM images of the sample. The main results agree with the RHEED observation. The film has 3D structures in zero- and low-dosed Cr areas and the film is flat at high Cr dosage. However, the structures in the zero- and low-dosed films are very different. While Cr-free FePt shows granular features without definite size or shape, and the grains look connected to each other, the low-dosed surface shows more regular shaped and smaller structures that are also separated from each other.

For our magnetism study, SMOKE was measured in the polar geometry, as shown in the third panel of Fig. 2. We measured square hysteresis loops where 3D structures were found. Considering we used the polar geometry, we can imagine that the structure of FePt is $L1_0$, since $L1_0$ FePt is known to have strong out-of-plane anisotropy due to its symmetry-breaking atomic structure along the surface normal direction. The value of H_c decreased with increased dosage of Cr, and a hard axis loop with zero remanence was measured at higher Cr dosage, which means that the magnetic easy axis is no longer along the normal direction. This suggests that the structure is not $L1_0$ and retains the disordered A1 phase. Cr addition to FePt is known to decrease H_c, so our result for large Cr dosage agrees with those of previous reports [20, 21]. However, the H_c value is higher in the low-dosed area than in Cr-free area, which means that a small dosage of Cr may help build $L1_0$, contrary to the effect of large dosage. And the shape of the loop is also squarer than that of the Cr free area, which can be explained by SEM images which show that the nanostructures in the low-dosed area are more regular in shape and size than those in the Cr-free area. Also, the magnetization direction switches within narrower range of reverse field in the low-dosed area than in Cr-free area. The last panel of Fig. 2 shows XMCD spectra for Fe after an external magnetic field was applied both along perpendicular and in-planar directions. XMCD spectra were measured both with normal incidence (0°) and oblique incidence (75°) of X-rays, which detects the magnetic moment parallel to the incident direction. Hence, only the normal components of the magnetic moments are detected with normal incident X-rays, while oblique incidence will give mostly the in-plane components of the magnetization. The results show zero- and low-dosed FePt has a magnetic easy axis perpendicular to the film, and large-dosed FePt has it in plane. An in-plane easy axis of the large-dosed area means that the structure is still in the disordered phase for which the anisotropy is mostly a result of the film shape.

The XMCD results are in accord with the SMOKE results. Both suggest that a large amount of Cr prohibits the phase transition from the disordered to ordered phase of FePt by stabilizing the disordered phase. Also, the magnetic easy axis is not perpendicular, while FePt nanoparticles in the small Cr dosed area have a perpendicular magnetic easy axis with a high H_c value.

To see how the phase of FePt is affected by Cr dosage, we have done SEM metrology at various Cr dosages for 0.05, 0.1, 0.15 and 0.3 nm of Cr (Fig. 3). At 0.05 nm dosage, part is composed of FePt nanostructures, however large areas look planar. With higher dosage, the area where the nanostructures reside gets smaller while the planar part become larger and gets interconnected. Around 0.3 nm of Cr dosage, most of it becomes planar phase (PP); only a small fraction of the film still remains in the island phase (IP). Since the area of the PP increases with the Cr dosage, the PP seems to have more Cr than the IP. This indicates that Cr atoms segregate from the island area to the planar area. The amount of Cr that can dissolve in FePt is limited, so the remaining Cr probably segregates

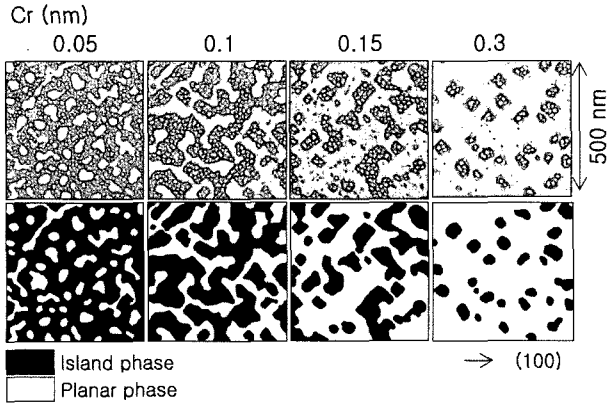

Fig. 3. SEM images (~x100 K) at various dosage of Cr on a 1.8-nm FePt film. Island phase and planar phase are highlighted with black and white in the pictures of the bottom row. The image size and crystalline direction are indicated in the figure.

into the planar region. Considering that the phase separation occurs in the 0-to-0.3 nm dosage range, which corresponds to two layers thickness of Cr, monolayer Cr on FePt seems to be energetically unstable. Kuo *et al.* reported that the addition of Cr inhibits grain growth and keeps the grain size small after a high temperature annealing, while the grain size of films without Cr becomes larger with annealing [21]. Our data as well shows the grain size is smaller than for films without Cr. In addition, the Cr dosage makes the grains round and disconnected from each other. We found there is a phase separation of the planar phase and island phases in the low Cr dosed area. This is believed due to Cr segregation which happens during the annealing.

We measured RHEED patterns for increasing annealing temperature to see how the surface of the sample changes with temperature (Fig. 4). Before annealing, the RHEED pattern shows blurred spots whose separation corresponds to one layer of the film. This means that the alloy is disordered, and the large spot size means that the surface is irregular and rough. As temperature increases, the RHEED streaks first sharpen, which shows that the surface get flatter and the crystalline structure improves. With higher temperature, superlattice spots begin to appear, which means $L1_0$ phase builds up. The RHEED results show that the surface first gets flatter and then the phase transition from disordered A1 to ordered $L1_0$ phase follows with a separation between the island phase and planar phase occurring.

Figure 5 shows an SEM image of the island phase in Cr dosed 3.6 nm (~10 stacks of Fe/Pt) FePt film after annealing at 550°C. The deposition method is the same as for the 1.8 nm film. In small dosages of Cr (0.2 nm), the

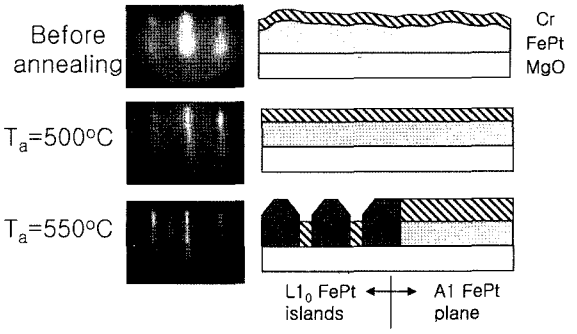

Fig. 4. Schematic diagram for nanostructure formation during annealing, and corresponding RHEED images. The films first flatten and then the IP and PP separate along with a segregation of Cr.

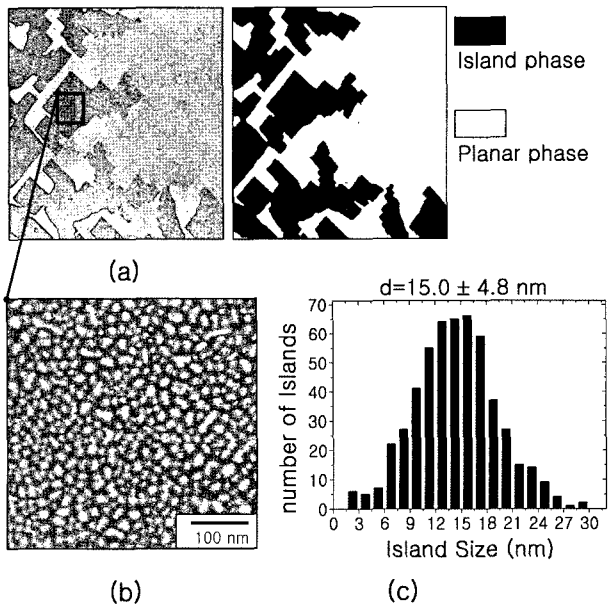

Fig. 5. (a) SEM image of a 0.2-nm Cr dosed 3.6-nm FePt film, (b) a zoomed-in image of the IP where the $L1_0$ FePt nanostructures are locate, and (c) histogram of the structure size counted in the area. The average value of the diameter is 15.0 nm and the standard deviation is 4.8 nm. The short dimensions correspond to non-circular islands.

surface of the film is composed of small nano structures surrounded by the planar phase. The size of the nanostructures is almost the same as those in the 1.8-nm film. In the 3.6-nm sample, however, we could get a larger total area of the IP than for the 1.8 nm one. This seems to be due to the better mobility of Cr in the 3.6 nm film, for the reason that the phase separation is thought due to Cr segregation. The island sizes were measured and we obtained a mono-dispersed Gaussian curve with 15-nm average size. The size and shape of the structures are not better than those obtained by chemical synthesis. However,

the distribution of dots is regular, since the structures are made from a uniformly deposited thin film. The film was grown epitaxially, so the symmetry axis of the $L1_0$ structure is fixed as is the magnetic easy axis, while the magnetic easy axis in chemical synthesized nanoparticles is usually random. The area of PP increases with Cr dosage and the IP disappears ~0.3 nm both in 1.8-nm and 3.6-nm films. Most of the boundary between the IP and PP is along <110> in Fig. 5(a). Since it is known that the {111} plane has minimum surface energy in the $L1_0$ phase, the boundary facets along <111> directions, and aligns the IP and PP boundary along the <110> [28]. This means that the PP boundary consists of ordered $L1_0$ phase rather than disordered Al phase.

SMOKE measurements in the polar geometry show that H_c decreases with Cr dosage. We measured XMCD of Fe with different Cr dosages and found there is an easy axis rotation, or spin reorientation transition (SRT) at ~0.3 nm dosage of Cr in the 1.8 nm FePt. Figure 6 shows the XMCD intensity which is proportional to the magnetic moment projection along the beam incident direction. It shows a crossing of the normal and in-plane components, which means that the magnetic easy axis is perpendicular to the film surface when the dosage is < 0.3 nm and become in-plane at higher dosage. The Cr dosage amount for the 3.6 nm FePt film was also measured and found to be about the same as for the 1.6 nm film. If the SRT is caused by Cr alloying with the FePt particles, the amount of Cr required for the SRT should double as the total amount of FePt doubles. However, this is not observed. The same amount of Cr triggers the SRT, which suggests that the SRT is mostly caused by the effect of Cr on the interface or surface that surrounds the boundary of the FePt nanoparticles. Perpendicular magnetic moments in the low-dosed area, which is contrary to the tendency of a shape anisotropy, means there exists a larger crystalline anisotropy which originates from the spin orbit interaction associated with the $L1_0$ order. As the Cr dosage increases, the structures remain in the A1 phase which only has shape anisotropy thus favoring in-plane anisotropy. Figure 6(c) shows the Fe XMCD spectra at 0.2-nm Cr dosage with normal incident x-rays and at 0.6-nm Cr with oblique incident x-rays for the 3.6-nm FePt sample. To compare in detail, we normalize to the L_2 peaks and see that the L_3 peak heights are different. Since the spin and angular moments are related via the sum and difference of the L_3 and L_2 XMCD intensities, a different peak ratio suggests that there is a structural difference in the FePt between the small and large Cr-dosed areas. Figure 6(d) is the XMCD of Cr, which shows that Cr is antiferromagnetically coupled with the Fe. Since Cr is antiferromagnetic the net moment is zero in its bulk, and the signal comes from the interface with FePt. The signal (after being normalized by the total Cr intensity) at 0.6-nm Cr is stronger than that for 0.2-nm Cr dosage. This indicates that the contact area of Cr to FePt is larger in the planar phase than in the island phase.

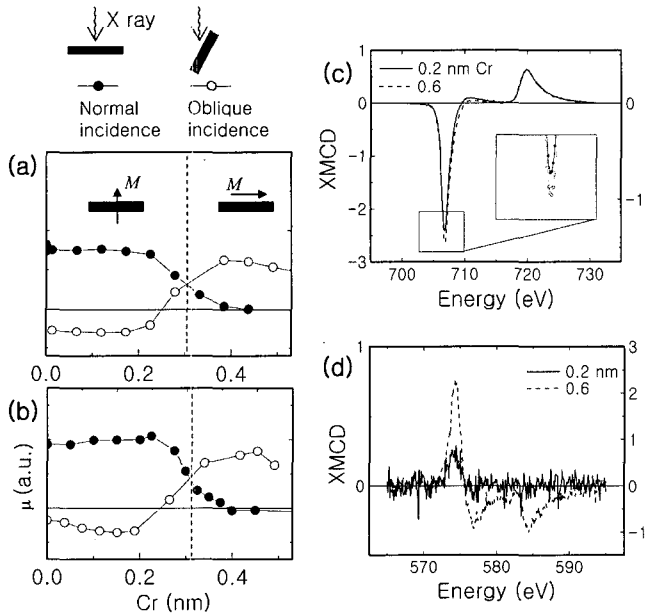

Fig. 6. Magnetic moment along normal and oblique (10 degree from surface) direction of (a) 1.8-nm sample and (b) 3.6-nm sample. Both show a spin reorientation transition (SRT) around 0.3-nm dosage of Cr. (c) Fe XMCD and (d) Cr XMCD before and after SRT.

The uniformly deposited film shows phase separation and we could find nano-size structures in the IP. But the position of the planar and island phases is not controllable. This problem can be overcome by doping Cr locally, for example by using artificial patterning of Cr. For this purpose we prepared a Cr-patterned MgO substrate. Circular and linear patterns were made by depositing 1.5 nm of Cr through a SiN contact mask made by e-beam lithography and chemical etching. The FePt was grown on the patterned substrate and the film was annealed at 550°C for 20 min. SEM images (Fig. 7) clearly show that there are different formations of FePt nanoparticles inside and outside of the pattern. Also, outside of the Cr pattern, the surface is different from a Cr-free surface, which suggests that Cr atoms diffuse outside the pattern. The image of the Cr-free surface was taken at a position several millimeters away from the pattern, so it is protected from Cr diffusion. The image shows a granular surface without a well defined size and shape. Since we use the same growth conditions for the FePt, the image is the same as that of the previously discussed sample [Fig. 2(a)]. The SEM

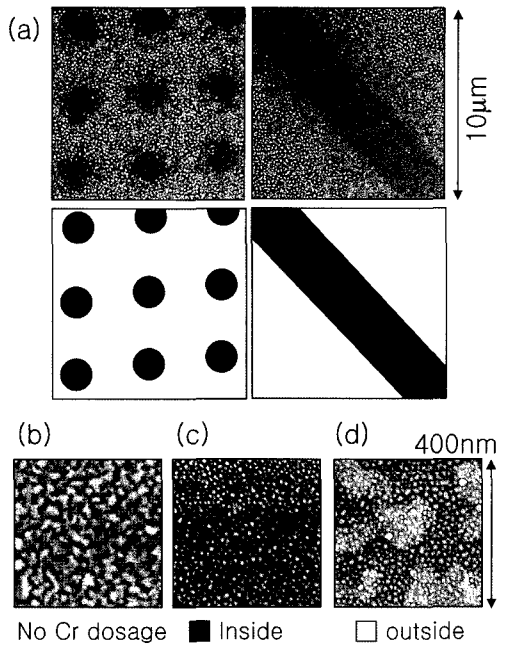

Fig. 7. (a) SEM images of FePt film grown on a Cr-patterned MgO substrate. Black and white shows the pattern design where only the black area has 1.5 nm Cr. SEM images of (b) Cr-free, (c) inside of pattern, and (d) outside of pattern. (b) was taken at least a millimeter away from the pattern. Figure (c) and (b) are different because Cr diffused outside of the pattern during annealing.

image outside of the Cr patterns shows nanostructures and also larger size structure, while the SEM image inside the pattern Cr shows only small structures. The SEM metrology for this patterned sample shows that intentional tailoring of islands is possible via artificial patterning of Cr.

4. Summary

We highlighted recent work at Argonne, given current interest in FePt. We have shown that small dosages of Cr to FePt have a major effect to make $L1_0$ FePt nanostructures: the size and the shape can be well controlled. The FePt has perpendicular easy axes, high coercivity, and square hysteresis loops. Cr is believed to facilitate the formation of round FePt islands and segregated planer A1 FePt. The separation into planar A1 phase of FePt and $L1_0$ FePt island phases occurs during annealing at ~550°C. Controlling the lateral region where nanostructures exist is possible via artificial pattering of Cr.

Acknowledgements

Part of this work was carried out at the Center for Nanoscale Materials at Argonne National Laboratory. The submitted manuscript has been created by UChicago Argonne, LLC, Operator of Argonne National Laboratory ("Argonne"). Argonne, a U.S. Department of Energy Office of Science Laboratory, is operated under Contract No. DE-AC02-06CH 11357. The U.S. Government retains for itself, and others acting on its behalf, a paid-up nonexclusive, irrevocable worldwide license in said article to reproduce, prepare derivative works, distribute copies to the public, and perform publicly and display publicly, by or on behalf of the Government.

References

[1] M. Yu, Y. Liu, A. Moser, D. Weller and D. J. Sellmyer, Appl. Phys. Lett. **20**, 3992 (1999).
[2] B. M. Lairson, M. R. Visokay, R. Sinclair, and B. M. Clemens, Appl. Phys. Lett. **62**, 639 (1993).
[3] A. Cebollada, D. Weller, J. Sticht, G. R. Harp, R. F. C. Farrow, R. F. Marks, R. Savoy and J. C. Scott, Phys. Rev. B **50**, 3419 (1994).
[4] M. R. Visokay and R. Sinclair, Appl. Phys. Lett. **66**, 1692 (1995).
[5] R. F. C. Farrow, D. Weller, R. F. Marks, M. F. Toney, A. Cebollada and G. R. Harp, J. Appl. Phys **79**, 5967 (1996).
[6] R. A. Ristau, K. Barmak, L. H. Lewis, K. R. Coffey, and J. K. Howard, J. Appl. Phys. **86**, 4527 (1999).
[7] T. Itoh, T. Kato, S. Iwata, and S. Tsunashima, IEEE Trans. Magn. **41**, 3217 (2005).
[8] Y. Huang. H. Okumura. G. C. Hadjipanayis, D. Weller, J. Magn. Magn. Mater. **242-245**, 317 (2002).
[9] T. Shima, T. Moriguchi, S. Mitani, K. Takanashi, H. Ito and S. Ishio IEEE Trans. Magn. **38**, 2791 (2002).
[10] S. Sun, C. B. Murray, D. Weller, L. Folks, and A. Moser, Science **287**, 1989 (2000).
[11] B. Rellinghaus, S. Stappert, M. Acet, and E. F. Wassermann, J. Magn. Magn. Mater. **266**, 142 (2003).
[12] Y. Sasaki, M. Mizuno, A. C. C. Yu, M. Inoue, K. Yazawa, I. Ohta, M. Takahashi, B. Jeyadevan, and K. Tohji, Magn. Magn. Mater. **282**, 122 (2004).
[13] Y. Zhang, J. Wan, M. J. Bonder, G. C. Hadjipanayis, and D Weller, J. Appl. Phys. **93**, 7175 (2003).
[14] A. C. C. Yu, M. Mizuno, Y. Sasaki, M. Inoue, H. Kondo, I. Ohta, D. Djayaprawira, and M. Takahashi, Appl. Phys. Lett. **82**, 4352 (2003).
[15] M. Chen, K. Kuroishi, and Y. Kitamoto, IEEE Trans. Magn. **41**, 3376 (2005).
[16] T. Saito, O. Kitakami, and Y. Shimada, J. Magn. Magn. Mater. **239**, 310 (2002).
[17] J. P. Liu, Y. Liu, C. P. Luo, Z. S. Shan, and D. J. Sellmyer, J. Appl. Phys **81**, 5644 (1997).
[18] M. F. Toney, W. Y. Lee, J. A. Hedstrom, and A. Kellock, J. Appl. Phys. **93**, 9902 (2003).
[19] T. Shima, T. Moriguchi, S. Mitani, and K. Takanashi,

Appl. Phys. Lett. **80**, 288 (2002).
[20] J. P. Chu, T. Mahalingam and S. F. Wang, J. Phys: Condens. Matter **16**, 561 (2004).
[21] P. C. Kuo, Y. D. Yao, C. M. Kuo, and H. C. Wu, J. Appl. Phys. **87**, 6146 (2000).
[22] Z. L. Zhao, J. S. Chen, J. Ding, Y. B. Yi, B. H. Liu and J. P. Wang, IEEE Trans. Magn. **41**, 3337 (2005).
[23] T. Maeda, T. Kai, A. Kikitsy, T. Nagase, and J. Akiyama, Appl. Phys. Lett **80**, 2147 (2002).
[24] C. J. Sun, G. M. Chow, and J. P. Wang, Appl. Phys. Lett. **82**, 1902 (2003).
[25] Y. Zhang, J. Wan, M. J. Bonder, G. C. Hadjipanayis, and D. Weller, J. Appl. Phys. **93**, 7175 (2003).
[26] J. Wan, Y. Huang, Y. Zhang, M. J. Bonder, G. C. Hadjipanayis, and D. Weller, J. Appl. Phys **97**, 10J121 (2005).
[27] T. Shima, K. Takanashi, Y. K. Takahashi, and K. Hono, Appl. Phys. Lett. **85**, 2571 (2004).
[28] T. Shima, K. Takanashi, Y. K. Takahashi and K. Hono, Appl. Phys. Lett. **88**, 063117 (2006).
[29] Y. Zhang, J. Wan, V. Skumryev, S. Stoyanov, Y. Huang, G. C. Hadjipanayis, and D. Weller, Appl. Phys. Lett. **85**, 5343 (2004).
[30] T. Shima, K. Takanashi, Y. K. Takahashi, K. Hono, G. Q. Li and S. Ishio, J. Appl. Phys. **99**, 033516 (2006).